

Controlling the Synaptic Plasticity of a Cu₂S Gap-Type Atomic Switch

Alpana Nayak,* Takeo Ohno, Tohru Tsuruoka, Kazuya Terabe, Tsuyoshi Hasegawa, James K. Gimzewski, and Masakazu Aono

It is demonstrated that a Cu₂S gap-type atomic switch, referred to as a Cu₂S inorganic synapse, emulates the synaptic plasticity underlying the sensory, short-term, and long-term memory formations in the human brain. The change in conductance of the Cu₂S inorganic synapse is considered analogous to the change in strength of a biological synaptic connection known as the synaptic plasticity. The plasticity of the Cu₂S inorganic synapse is controlled depending on the interval, amplitude, and width of an input voltage pulse stimulation. Interestingly, the plasticity is influenced by the presence of air or moisture. Time-dependent scanning tunneling microscopy images of the Cu-protrusions grown in air and in vacuum provide clear evidence of the influence of air on their stability. Furthermore, the plasticity depends on temperature, such that a long-term memory is achieved much faster at elevated temperatures with shorter or fewer number of input pulses, indicating a close analogy with a biological synapse where elevated temperature increases the degree of synaptic transmission. The ability to control the plasticity of the Cu₂S inorganic synapse justifies its potential as an advanced synthetic synapse with air/temperature sensibility for the development of artificial neural networks.

1. Introduction

To build a machine with a human level of intelligence is an age-old dream of mankind. In his famous 1950 paper on computing machinery and intelligence,^[1] Alan Turing admitted “we can only see a short distance ahead, but we can see plenty

there that needs to be done”. Despite over half a century of effort, modern state-of-the-art von-Neumann computers^[2] have not overpowered the brain's capability in many computational tasks, such as visual perception in complex environments. The achievements of CMOS architecture are indeed impressive, but the performance of these computers are plagued by a speed-limiting step known as the von-Neumann bottleneck^[3] together with orders of magnitude more energy and space consumption compared to their biological counterparts. In an attempt to match the efficiency of biological systems, artificial neural network architecture has been conceived^[4] in which logic circuits dynamically reconfigure in response to inputs, like a human brain.^[5] Basically, nanoscale electronic devices that can perform non-volatile logic,^[6] multilevel,^[7] and memristive^[8] operations with inherent learning abilities are desired.

So far, resistive switching (RS) devices using different materials, such as metal oxides and chalcogenides, and different architectures have shown the potential to mimic biological synaptic behavior.^[9,10] In metal oxide-based systems,^[11,12] oxygen vacancies are responsible for the RS operation and the output conductance depends on the history of switching events, thereby causing the memory effect.^[13] In the chalcogenide glass-based system, phase change of the material is responsible for the RS operation.^[14] This system demonstrates an interesting aspect of synaptic behavior, namely, the spike-timing-dependent plasticity (STDP) underlying Hebbian learning.^[15] STDP has also been demonstrated using hybrid materials^[16] and hybrid nanocrossbar/CMOS architecture including a Ag-incorporated Si active layer.^[17] Recently, we discovered that a Ag₂S chalcogenide-based gap-type atomic switch, which is an exciting subset of RS devices, demonstrates a number of fascinating synaptic properties, including learning^[18] and memorization.^[19,20] Because of its unique operating mechanism, composed of metal filament formation/annihilation, the atomic switch shows exotic behaviors^[21] such as quantized conductance multistate switching^[22] in addition to the conventional memristive operations.^[23] Unlike some strictly non-volatile RS devices, the atomic switch exhibits time-dependent conductance, which has lead to the observation of short-term (volatile) and long-term (non-volatile) memories.

Dr. A. Nayak, Dr. T. Ohno, Dr. T. Tsuruoka, Dr. K. Terabe, Dr. T. Hasegawa, M. Aono
International Center for Materials Nanoarchitectonics (WPI-MANA) National Institute for Materials Science (NIMS)
1-1 Namiki, Tsukuba, 305-0044, Japan
E-mail: NAYAK.Alpana@nims.go.jp



Prof. J. K. Gimzewski
Department of Chemistry and Biochemistry
University of California
Los Angeles
607 Charles E. Young Drive East, Los Angeles, CA 90095, USA
Prof. J. K. Gimzewski
California NanoSystems Institute (CNSI)
University of California
Los Angeles, 570 Westwood Plaza, Los Angeles, CA 90095, USA

DOI: 10.1002/adfm.201200640

Inspired by the exciting synaptic properties of the Ag_2S atomic switch, Stieg et al. proposed a new hardware-based architecture utilizing a self-assembled Ag_2S -atomic switch network that aims to harness the power of highly coupled, nonlinear systems in neuromorphic computation.^[3]

Although the idea of using RS devices to emulate neural synaptic behavior is not new, endeavors continue to identify materials and architectures that can bring electronics closer to the complexity of the human brain. We believe that different systems, even with slight variations in operation based on materials/architectures, can be rewarding when put together to design elements for the complex circuitry of the brain. It goes without saying that the brain's complexity arises from unity in diversity. As a simple example, various metal ions (Fe, Zn, Cu, etc.) influence the process of neural signal transmission, yet each has a different role; for instance, the flow of Cu in the brain has a recognized role in learning and memory.^[24]

Our previous reports^[19,20] demonstrated the synaptic behavior of a Ag_2S gap-type atomic switch; however, the synaptic behavior of a Cu_2S gap-type atomic switch has not been explored so far. In this paper, we demonstrate the synaptic behavior of a Cu_2S gap-type atomic switch and show that the synaptic plasticity can be controlled not only by input voltage pulse stimulation, but also by the presence of air (or moisture) and by temperature. Apart from the reasonably higher operation voltage, the effect of air (or moisture) marks an important material-based difference between the Cu_2S and previously reported Ag_2S systems. Moreover, this is the first study on the temperature dependence of synaptic behavior revealing a close analogy to the behavior of a biological synapse at elevated temperatures and is crucial for any practical implementation. These results indicate the possibility of advanced applications of the Cu_2S gap-type atomic switch, exhibiting synaptic behavior with sensibility for air (or moisture) and temperature, for the development of artificial intelligent machines.

2. Results and Discussion

Firstly, the analogy between a biological synapse and a Cu_2S gap-type atomic switch is discussed briefly. **Figure 1a** shows a schematic illustration of a biological synapse. The arrival of an action potential at the pre-synaptic neuron releases neurotransmitters at the synapse which bind with the receptors of the post-synaptic neuron to form ion channels for signal transmission. Consequently, an enhancement of the synaptic potential occurs, which can last for a fraction of a second to hours or even longer depending on the rate of stimulation. For instance, a frequent stimulation by action potential causes long-term enhancement in the synaptic connection (weight).^[25,26] This is called synaptic plasticity and is believed to be the basis of sensory memory (SM), short-term memory (STM), and long-term memory (LTM) described in the psychological memorization model of human brain.^[27] **Figure 1b** shows the construction of a Cu_2S gap-type atomic switch using a Cu_2S solid electrolyte grown on a Cu electrode and a counter Pt electrode with a nanogap made between them by a scanning tunneling microscope.^[28] When a voltage is applied between the electrodes such that the Cu_2S is at positive bias, the Cu^+ ions, which were uniformly distributed at the

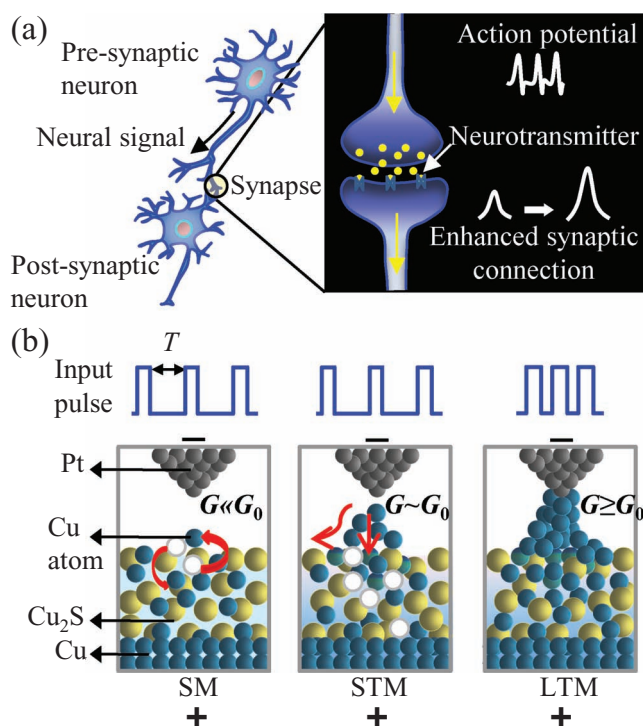


Figure 1. a) In a biological synapse, the arrival of an action potential releases neurotransmitters that assist ion channels for signal transmission. Frequent stimulation by action potential results in a persistent increase in the synaptic connection. b) Schematic illustration of a Cu_2S gap-type atomic switch (referred to as a Cu_2S inorganic synapse) in sensory memory (SM), short-term memory (STM), and long-term memory (LTM) states depending on the interval (T) of the input voltage pulse stimulation. The conductance (G) for a single atomic contact is given by $G_0 = 77.5 \mu\text{S}$.

initial state, diffuse toward the sub-surface of Cu_2S . Depending on the applied voltage and the thermodynamic conditions (e.g., temperature), the Cu^+ ions precipitate to form Cu atoms on the surface due to a solid electrochemical reaction $\text{Cu}^+ + e^- \rightarrow \text{Cu}$. Subsequently, the precipitated Cu atoms form a bridge between the electrodes and the conductance increases. The conductance corresponding to a single atomic contact is given by $G_0 = 2e^2/h = 77.5 \mu\text{S}$, where e is the electron charge and h is Planck's constant. The change of conductance of the Cu_2S gap-type atomic switch is considered analogous to the change of strength of a biological synaptic connection underlying synaptic plasticity. Thus, the Cu_2S gap-type atomic switch is referred to as a Cu_2S inorganic synapse hereafter.

As illustrated in **Figure 1b**, the Cu_2S inorganic synapse exhibits three different conductance states analogous to the SM, STM, and LTM states in the human brain. Our understanding of such states was already presented in previous reports on the Ag_2S system.^[19,20] While Ag_2S is an n -type material, the Cu_2S is a p -type material (more correctly described as $\text{Ag}_{2+\delta}\text{S}$ and $\text{Cu}_{2-\delta}\text{S}$, respectively). In Cu_2S , the Cu vacancies act as electron acceptors and give rise to free holes for conductivity; therefore, the resistance of Cu_2S is known to increase with increasing Cu concentration.^[29] It should be mentioned here that during synapse operation the change in resistance of the Cu_2S material

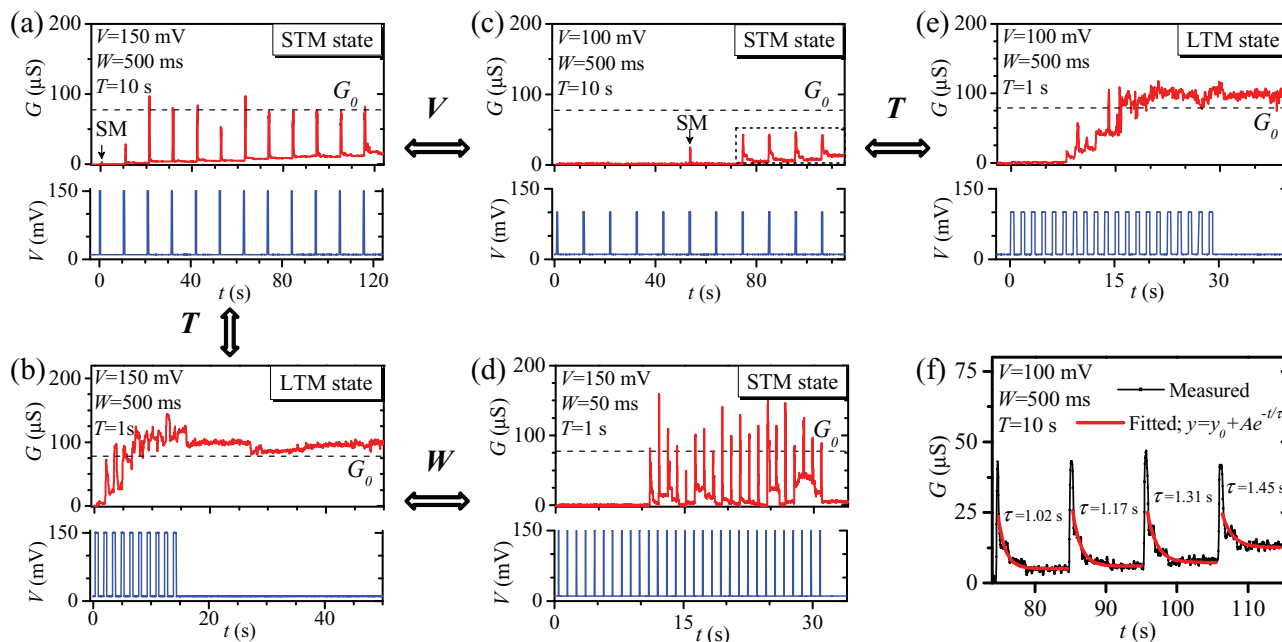


Figure 2. Changes in the conductance (G) of a Cu₂S inorganic synapse in vacuum at room temperature depending on the interval (T), amplitude (V), and width (W) of the input voltage pulse stimulation: a) $V=150$ mV, $W=500$ ms, $T=10$ s; b) $V=150$ mV, $W=500$ ms, $T=1$ s; c) $V=100$ mV, $W=500$ ms, $T=10$ s; d) $V=150$ mV, $W=50$ ms, $T=1$ s; and, e) $V=100$ mV, $W=500$ ms, $T=1$ s. f) The values of time constant (τ) extracted from the fits of the conductance decay curves shown in the dashed rectangular box in (c). An exponential function, $y = y_0 + A e^{-t/\tau}$, was used to fit the conductance curves.

itself due to the local Cu⁺ enrichment at the subsurface should be negligible taking into account the much larger resistance of the nanogap, since the Cu₂S inorganic synapse is basically a Cu₂S gap-type atomic switch. Briefly, in the SM state, small precipitation occurs that increases the conductance by a small amount ($\ll G_0$) only during the pulse application and the information of the input is stored as an increase in the concentration of Cu⁺ ions at the Cu₂S subsurface. In the STM state, small and unstable nuclei of precipitated Cu atoms cause unstable bridging, probably due to surface diffusion or reincorporation of Cu atoms into the Cu₂S electrolyte to balance the energetics at the interface. Hence, a persistent conductance of approximately G_0 is not achieved. In the LTM state, the Cu₂S subsurface is enriched with Cu⁺ ions, which makes the precipitated Cu atoms more stable against reincorporation, forming a complete and robust atomic bridge. Eventually, a Cu cluster forms, enhancing the stability and retention of the conductance of approximately G_0 . The stability of a metal cluster with a magic number of valence electrons is well known in the field of photography,^[30] and might be applicable to explain the stability of the LTM state.

In the following subsections, the dependence of these conductance states on the input voltage pulse, the influence of air (or moisture), and the effect of temperature are presented.

2.1. Stimulation by Input Voltage Pulse

Figure 2a,b show the changes in conductance of the Cu₂S inorganic synapse obtained in vacuum for input voltage pulses of

amplitude (V) = 150 mV, width (W) = 500 ms, and intervals (T) = 10 and 1 s, respectively. For $T=10$ s, the conductance reached approximately G_0 during most of the input pulses, but it decayed spontaneously in the interval between the pulse applications, indicating an STM state (Figure 2a). Note that, during the first input pulse, an SM state was observed (Figure 2a) which is contrary to other memristive devices whose output always changes with every input.^[8,11] For $T=1$ s, a long lived transition to the higher conductance state ($\geq G_0$ for at least 20 s) was achieved after the last input pulse, which corresponds to a LTM state (Figure 2b). The dependence of the conductance states on the input pulse amplitude obtained in vacuum are shown in Figure 2c and e for $T=10$ and 1 s, respectively. For the input pulse with the original $T=10$ s and $W=500$ ms but a smaller $V=100$ mV (Figure 2c), an SM state was observed at the 6th pulse prior to the observation of the first STM state at the 8th pulse. For the input pulse with the original $T=1$ s and $W=500$ ms but a smaller $V=100$ mV (Figure 2e), the first STM state was achieved after 5 input pulses and a higher conductance state was achieved after 11 input pulses. Figure 2f shows the fitting of the conductance curves of the successive STM states shown within a dashed rectangular box in Figure 2c. An exponential decay function, $y = y_0 + A e^{-t/\tau}$, was used where y is the conductance, y_0 is the conductance offset, A is the fit constant, τ is the time constant, and t is the time after each input pulse application. It should be mentioned here that among the several decay functions known in psychology, exponential functions are the most commonly used for the quantitative description of retention of human memory.^[31] The increasing values of τ for the successive curves indicate that the decay of conductance

maintains a history of previous inputs depending on the non-stoichiometry and rearrangements of Cu^+ ions at the subsurface of Cu_2S . A similar effect can also be seen in Figure 2a, together with a steep fall of conductance instantaneously at the end of each pulse indicating the effect of electric field. The dependence of the conductance state on the input pulse width obtained in vacuum is shown in Figure 2d. For the input pulse with the original $V = 150$ mV and $T = 1$ s but a narrower width $W = 50$ ms, the first STM state was achieved after 10 input pulses and a LTM state was not achieved even after 30 input pulses. Thus, the SM, STM, and LTM states of the Cu_2S inorganic synapse depend on the input voltage pulse stimulation, similar to the Ag_2S inorganic synapse.^[19,20] However, the operation voltage of the Cu_2S inorganic synapse is a reasonable amount higher than that of the Ag_2S inorganic synapse. This is consistent with the previously reported relatively higher voltage needed for the switching operation of the Cu_2S gap-type atomic switch compared to that of the Ag_2S gap-type atomic switch.^[28,32,33]

2.2. Effect of Air or Moisture

The most significant difference between the Ag_2S and Cu_2S inorganic synapses was found in the effect of ambient conditions. For the Ag_2S system, there was no influence of air (or moisture) on operation; as a result, almost the same behavior was observed under both ambient and vacuum conditions. On the other hand, the operation of Cu_2S inorganic synapse was influenced by the presence of air (relative humidity $\approx 50\%$). Compared to its operation in vacuum for the same input pulse condition (Figure 2a), the values of conductance were significantly higher after the application of each pulse when operated in air (Figure 3a). It is noteworthy that these values of conductance, though below G_0 , were maintained for a long time after the pulse application. Figure 3b shows one such example of conductance state below G_0 observed over 30 s after a single input pulse in air. The fitting of the conductance curve using $y = y_0 + A e^{-t/\tau}$ yielded a value of τ of 5 s, which is much larger than those obtained in vacuum (Figure 2f). Though the decay of conductance might have a different origin, the value of τ indicates a qualitative difference in the stability of conductance between air and vacuum. To confirm this difference, we carried

out time-dependent scanning tunneling microscopy imaging of the Cu protrusions grown on Cu_2S in air and in vacuum.

Figure 4 shows images of the Cu_2S surface in air before and after growing a Cu protrusion. Because the surface of Cu_2S was rough, a slow scanning with a relatively large sample bias was preferred and a large protrusion needed to be grown that could be easily identified. To grow the protrusion, a voltage pulse of $V = 200$ mV and $W = 2$ s was applied and the scanning tunneling microscope-feedback loop was kept active such that the tip could retract following the growth. All imaging was carried out at a sample bias of -100 mV, a set point tunneling current of 1 nA, and a scan speed of 500 nm s^{-1} . Note that there is a time gap between the moment at which the protrusion was grown and the moment at which the image of the protrusion was obtained due to the time required for imaging.^[34] The image of the surface of Cu_2S before the pulse application is shown in Figure 4a wherein the point at which the pulse was applied is marked by a circle. The next image of the same region, obtained 8 min after the pulse application, shows a clear Cu cluster (Figure 4b). Successive imaging revealed that the Cu cluster was quite stable. The image obtained 48 min after pulse application (Figure 4c) shows the remaining part of the cluster. Figure 4d shows the height profiles corresponding to the lines drawn across the protrusion-grown region in Figure 4a–c. As can be seen, a cluster about 12 nm high and 30 nm wide was obtained after 8 min, which shrank to about 4 nm high and 10 nm wide after 48 min. On the contrary, the Cu protrusion grown in vacuum under the same voltage pulse condition was found difficult to image due to fast shrinking.

Figure 5a,b show typical examples of the images of Cu_2S surface in vacuum before and 5 min after the same pulse application as in Figure 4. Although a protrusion of almost the same height grew, as was indicated by the tip retraction during growth, only remnants of it could be imaged after just 5 min. A change in morphology of the region of pulse application (marked by dashed circles in the 3D representations) can be seen, which is evident of these remnants. The height profiles corresponding to the lines drawn on the 2D images (Figure 5c) show an increased roughness by about 1 nm only, indicating the fast dissolution of the grown protrusion in vacuum. It should be mentioned here that the sample bias of -100 mV while imaging may be sufficient to induce electrochemical dissolution. The fact that a

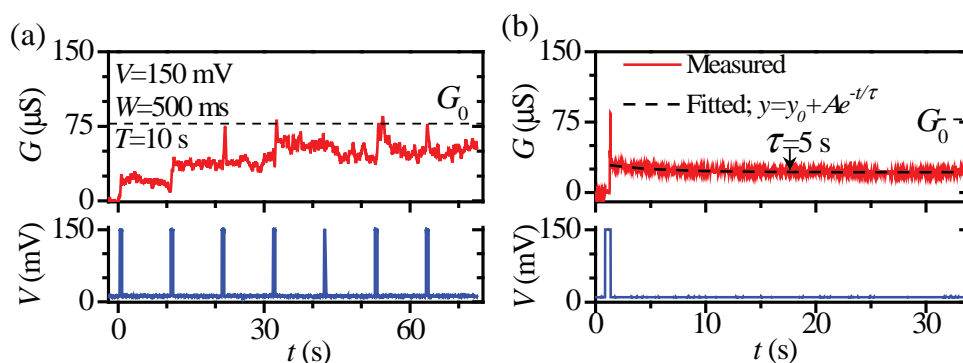


Figure 3. Change in conductance (G) under ambient conditions for: a) multiple inputs of a voltage pulse of amplitude (V) 150 mV and width (W) 500 ms at an interval (T) of 10 s, and, b) a single input of the same pulse. The time constant (τ) is obtained from the fit (dashed curve) of the conductance curve using the exponential function $y = y_0 + A e^{-t/\tau}$.

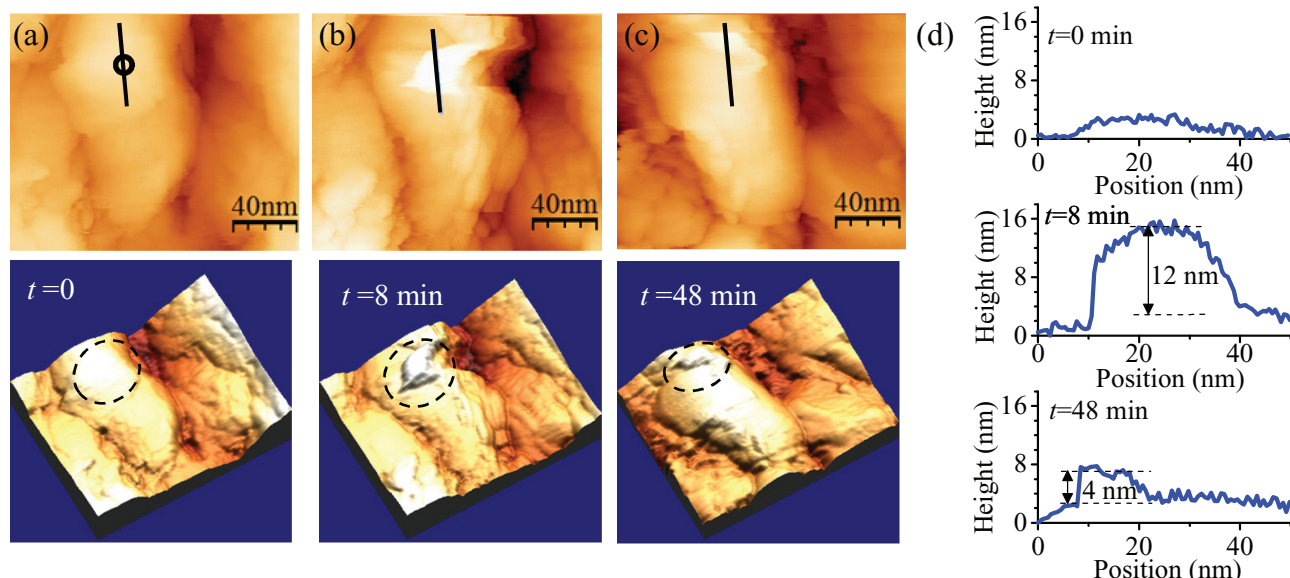


Figure 4. Scanning tunneling microscopy images of a Cu protrusion grown in air on the Cu_2S surface upon application of a pulse of 200 mV for 2 s: a) Before application of the pulse at the point marked by a circle, and, b) 8 min and c) 48 min after application of the pulse. Both 2D and 3D representations of the images are shown (one below the other for clarity). d) Height profiles corresponding to the lines drawn on the 2D images across the protrusion grown region.

significant part of the Cu protrusion survived in air under this sample bias (Figure 4) is evident of its enhanced stability.

In order to obtain an image of the Cu protrusion in vacuum, a voltage pulse of longer width was applied. **Figure 6a–c** show the successive images of the Cu_2S surface obtained in vacuum before and after growing a Cu protrusion with a pulse of the same amplitude but a longer $W = 4$ s. A cluster of smaller size, compared to that grown in air (Figure 4b), could be imaged 5 min after the pulse application (Figure 6b). The image of the same region 12 min later shows further reduced size of the cluster (Figure 6c), and thereafter the cluster was hardly visible. Figure 6d shows the height profiles corresponding to the lines drawn across the protrusion growing region in Figure 6a–c. The

height of the protrusion was about 5 nm after 5 min, shrinking to about 2 nm after 12 min from pulse application. Note that, despite the wider pulse of $W = 4$ s which might have caused a bigger protrusion compared to that grown in air for $W = 2$ s (Figure 4b), a smaller cluster was imaged in vacuum, enriching the evidence for the fast dissolution. Thus, the time-dependent imaging clearly revealed that the Cu protrusion in air is more stable than in vacuum.

Generally, the atoms in a cluster rearrange to attain the energetically most favorable symmetry isomer of the cluster. The special stability for clusters containing certain number of atoms is known in the literature based on the fascinating concept of magic number.^[30] However, the stability of such clusters on a

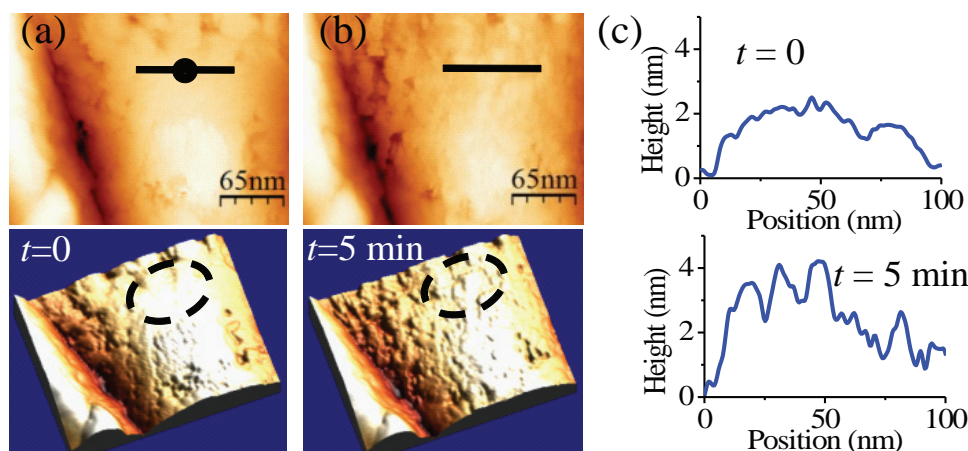


Figure 5. Scanning tunneling microscopy images of Cu_2S surface in vacuum: a) before and b) 5 min after application of the same voltage pulse as in Figure 4 at the point marked by a circle. (c) The height profiles corresponding to the lines drawn on the 2D images.

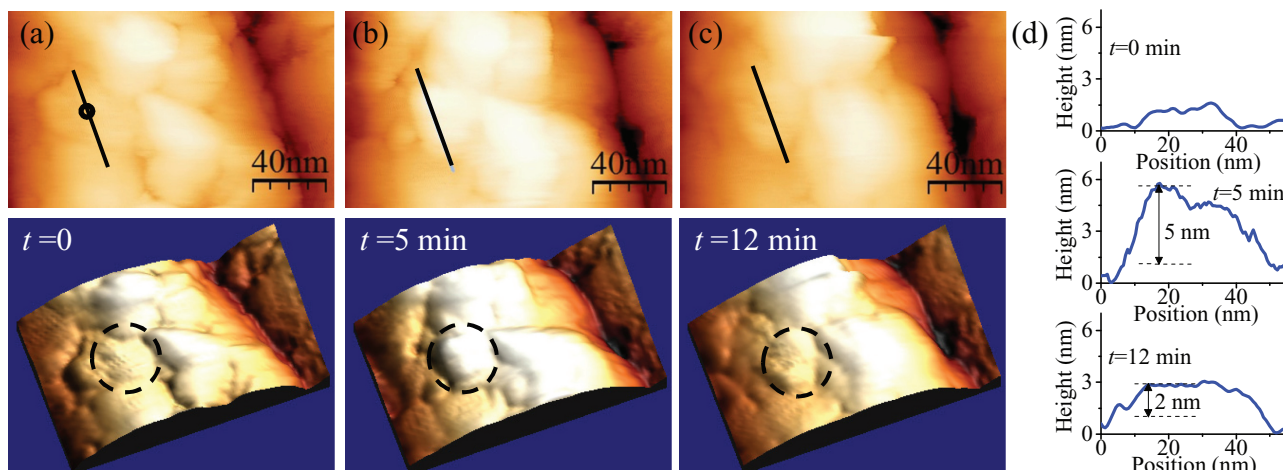


Figure 6. Scanning tunneling microscopy images of Cu-protrusion grown in vacuum on Cu_2S surface upon application of the same voltage pulse as in Figure 4 but for a longer width of 4 s: a) before application of the pulse at the point marked by a circle and b) 5 min; c) 12 min after application of the pulse. d) Height profiles corresponding to the lines drawn on the 2D images.

surface may be limited or time-dependent. We suggest that, in vacuum, the stability of a Cu cluster is limited mainly by surface diffusion and reincorporation. In air, additional factors depending on the atmosphere influence the stability; for instance, the chemisorption of oxygen^[35] and water^[36] can form energetically stable clusters of copper oxides and hydroxides. Since these are charge-transfer processes, open electronic shell clusters with a low ionization potential should be more reactive than closed shell clusters. Such reactions are spontaneous and have also been reported to show a strong dependence on the cluster size.^[37] In our study, the observation of the time-dependent stability of Cu clusters in air is consistent with a previous report in the literature;^[38] however, the dependence of stability on the cluster size itself will be a topic of future research. These observations open a new perspective for further investigations of air-exposed Cu nanoclusters for exploring stable conductance states exhibiting LTM with a value less than G_0 . This is the first time-dependent scanning tunneling microscope observation of Cu protrusions on Cu_2S that provides direct evidence with respect to stability; the results indicate the possibility of achieving advanced operation with the ability to sense the atmosphere.

2.3. Effect of Temperature

The temperature dependence of the Cu_2S inorganic synapse was studied in vacuum for two different width ($W = 500$ and 50 ms) of the same input pulse of $V = 150$ mV and $T = 1$ s. **Figure 7a** shows the conductance states measured at various temperatures for the input pulses of $W = 500$ ms. At room temperature ($\text{RT} \approx 22^\circ\text{C}$), the conductance reached a maximum of G_0 during single input pulse and decayed back to its initial value immediately after the pulse application, indicating a SM state. At 30°C , a STM state was achieved for a single input pulse, but at least 3 pulses were required for the formation of a LTM state. However, at 40°C , a single input pulse was enough to achieve

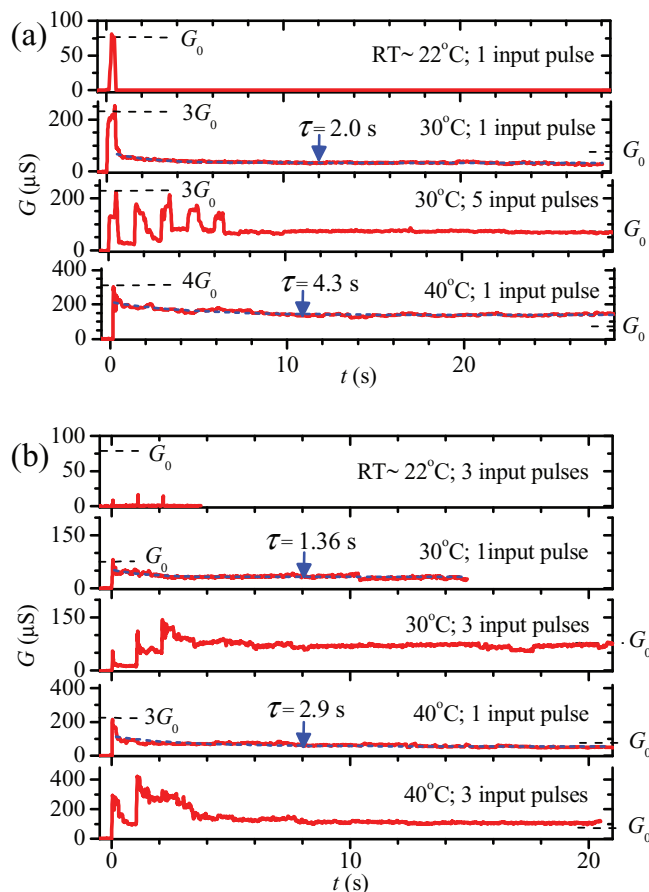


Figure 7. Temperature dependence of conductance (G) of a Cu_2S inorganic synapse in vacuum for input voltage pulses of amplitude = 150 mV, interval = 1 s, and width = 500 ms (a) and 50 ms (b). RT is room temperature. The values of time constant (τ) are extracted from the fits (dashed curves) of the conductance decay curves using the exponential function $y = y_0 + A e^{-t/\tau}$.

a LTM state. It is to be noted that, during the pulse application, the values of conductance at 30 °C ($\approx 3 G_0$) and at 40 °C ($\approx 4 G_0$) were higher than at RT ($\approx G_0$). The values of τ obtained from the exponential fits also increased with increasing temperature, indicating a better maintenance of synaptic strength analogous to a biological synapse at elevated temperatures. Thus, a LTM state could be obtained with fewer number of input pulses at elevated temperatures compared to that at RT under the same pulse condition, as shown in Figure 2b.

Figure 7b shows the conductance states measured under similar conditions but with a narrower width ($W = 50$ ms) of the input pulse. At RT, a SM state with a conductance of approximately $0.2 G_0$ during the pulse was observed. At 30 °C, a STM state was achieved for a single input pulse, but 3 pulses were required for the formation of a LTM state. At 40 °C, a single input pulse also yielded a STM state but with a higher value of conductance (approximately $3 G_0$) than at 30 °C (approximately G_0). For the formation of a LTM state at 40 °C, at least 2 pulses were required. Not only the values of conductance but also the values of τ extracted from the exponential fits increased with temperature. Thus, a LTM state was obtained with a narrower pulse width at elevated temperatures, while at RT (Figure 2d) an LTM state was not achieved even after 30 inputs of the same pulse condition. On the basis of these observations, we suggest an increased precipitation of Cu atoms at an elevated temperature. The rate of precipitation can be significantly enhanced at these temperatures since it depends exponentially on the tunneling current flowing through the inorganic synapse.^[39] The behavior of the inorganic synapse at elevated temperature is consistent with our previous observation of the exponentially faster switching of the Cu_2S gap-type atomic switch with increasing temperature.^[28]

In biology, the temperature change is known to have a major impact on the function of the central nervous system.^[40] The biological synaptic transmission that involve the integrated functioning of multiple factors might be differentially influenced by a temperature change.^[41] Studies have shown that a large increase in amplitudes of facilitation and augmentation and little change in the amplitude of depression at higher temperatures dramatically improve the maintenance of synaptic strength.^[42] Although a direct correlation with the biological system is not possible at this stage, our system of Cu_2S inorganic synapse shows close analogy as it exhibits a large increase in conductance and a significant increase in time constant of the conductance decay curves at higher temperatures, facilitating faster LTM formation with fewer or shorter stimulations (Figure 7a,b). In addition, the successful technological implementation of the Cu_2S inorganic synapse would also demand its ability to operate above RT. More importantly, because of its response to temperature and air, this system can be regarded as an advanced artificial synapse with the potential to perceive environment, like the human brain.

3. Conclusions

We demonstrated that a Cu_2S inorganic synapse mimics the key features of learning and memorization in the human brain, namely, SM, STM, and LTM states. The synaptic plasticity

underlying these states can be controlled not only by the input voltage pulse stimulation but also by the presence of air (or moisture) and temperature. The sensibility of the Cu_2S inorganic synapse toward air or moisture marks a significant material-based difference from the previously reported Ag_2S inorganic synapse. This is the first temperature-dependence investigation of the atomic switch-based inorganic synapse, suggesting a close analogy with a biological synapse since both show a better maintenance of synaptic strength at elevated temperatures. Our study indicates the possibility of achieving advanced artificial synapse element with the ability to sense two important environmental factors, viz. temperature and air. Nevertheless, the uniqueness of the human brain is its ability to perceive environment. It is expected that, together with the emerging devices such as metal-oxide memristors and phase-change memories, our inorganic synapses based on the concept of atomic switch using different materials will contribute to the development of artificial neural networking systems.

4. Experimental Section

The Cu_2S inorganic synapse, which is basically a Cu_2S gap-type atomic switch, consisted of a Cu_2S solid electrolyte on a Cu electrode and a counter Pt electrode (ion-blocking) separated from each other by a nanogap. A scanning tunneling microscope was used to make the nanogap by positioning the Pt tip above the Cu_2S surface with a sample bias of 10 mV and a set point tunneling current of 1 nA. The existence of the gap was confirmed by the exponential relation of tunneling current with gap distance as well as by the observation of Cu protrusion grown on the surface of the Cu_2S electrolyte.^[28,34] The Cu_2S electrolyte was prepared by sulfurizing a Cu-plate in sulfur vapor at 80 °C for 5 min in an evacuated glass ampoule. The details of the sample preparation and its characterization have been presented elsewhere.^[28] The conductance measurements were carried under ultra high vacuum (10^{-7} Pa) as well as in air. The initial conductance state of each measurement was adjusted to 0.1 μS . The input voltage pulses were applied using a conventional pulse generator (WF1946) and the output conductance was measured, using a semiconductor parameter analyzer (Agilent 4155C), by recording the output voltage across a series-connected reference resistance of 10 k Ω .^[19] The change of conductance after the pulse application was measured at a sample bias of +10 mV, which is small enough not to induce any electrochemical reaction. Measurements at elevated temperatures were accomplished by indirect resistive heating of the sample.^[28]

Acknowledgements

Part of this work was conducted under the Key-Technology Research Project, "Atomic Switch Programmed Device", supported by the MEXT, and the Strategic Japanese-German Cooperative Program, "Faradaic currents and ion transfer numbers in electrochemical atomic switches", supported by JST.

Received: March 7, 2012
Published online: May 25, 2012

- [1] A. M. Turing, *Mind: Q. Rev. Psychol. Philos.* **1950**, *LIX*, 433.
- [2] J. von Neumann, *IEEE Ann. Hist. Comp.* **1988**, *10*, 243.
- [3] A. Z. Stieg, A. V. Avizienis, H. O. Sillin, C. Martin-Olmos, M. Aono, J. K. Gimzewski, *Adv. Mater.* **2012**, *24*, 286.
- [4] S. Thakoor, A. Moopenn, T. Daud, A. P. Thakoor, *J. Appl. Phys.* **1990**, *67*, 3132.

- [5] G. Indiveri, E. Chicca, R. Douglas, *IEEE Trans. Neural Networks* **2006**, 17, 211.
- [6] T. Hanyu, S. Aragaki, T. Higuchi, *IEEE Proc. Circuits Dev. Syst.* **1995**, 142, 165.
- [7] A. Beck, J. G. Bednorz, Ch. Gerber, C. Rossel, D. Widmer, *Appl. Phys. Lett.* **2000**, 77, 139.
- [8] D. B. Strukov, G. S. Snider, D. R. Stewart, R. S. Williams, *Nature* **2008**, 453, 80.
- [9] D. B. Strukov, H. Kohlstedt, *MRS Bull.* **2012**, 37, 108.
- [10] M. Versace, B. Chandler, *IEEE Spectrum*, **2010**, <http://spectrum.ieee.org/robotics/artificial-intelligence/moneta-a-mind-made-from-memristors/0> (accessed May 2012).
- [11] J. J. Yang, M. D. Pickett, X. Li, D. A. A. Ohlberg, D. R. Stewart, R. S. Williams, *Nat. Nanotechnol.* **2008**, 3, 429.
- [12] K. Seo, I. Kim, S. Jung, M. Jo, S. Park, J. Park, J. Shin, K. P. Biju, J. Kong, K. Lee, B. Lee, H. Hwang, *Nanotechnology* **2011**, 22, 254023.
- [13] T. Chang, S.-H. Jo, W. Lu, *ACS Nano* **2011**, 5, 7669.
- [14] D. Kuzum, R. G. D. Jeyasingh, B. Lee, H. -S. P. Wong, *Nano Lett.* **2012**, 12, 2179.
- [15] G. Bi, M. Poo, *J. Neurosci.* **1998**, 18, 10464.
- [16] Q. Lai, L. Zhang, Z. Li, W. F. Stickle, R. S. Williams, Y. Chen, *Adv. Mater.* **2010**, 22, 2448.
- [17] S. H. Jo, T. Chang, I. Ebong, B. B. Bhadviya, P. Mazumder, W. Lu, *Nano Lett.* **2010**, 10, 1297.
- [18] T. Hasegawa, T. Ohno, K. Terabe, T. Tsuruoka, T. Nakayama, J. K. Gimzewski, M. Aono, *Adv. Mater.* **2010**, 22, 1831.
- [19] T. Ohno, T. Hasegawa, T. Tsuruoka, K. Terabe, J. K. Gimzewski, M. Aono, *Nat. Mater.* **2011**, 10, 591.
- [20] T. Ohno, T. Hasegawa, A. Nayak, T. Tsuruoka, J. K. Gimzewski, M. Aono, *Appl. Phys. Lett.* **2011**, 99, 203108.
- [21] T. Hasegawa, K. Terabe, T. Tsuruoka, M. Aono, *Adv. Mater.* **2012**, 24, 252.
- [22] K. Terabe, T. Hasegawa, T. Nakayama, M. Aono, *Nature* **2005**, 433, 47.
- [23] T. Hasegawa, A. Nayak, T. Ohno, K. Terabe, T. Tsuruoka, J. K. Gimzewski, M. Aono, *Appl. Phys. A* **2011**, 102, 811.
- [24] F. Arnesano, in *Ideas in Chemistry and Molecular Sciences: Where Chemistry Meets Life.*, (Ed: B. Pignataro), Wiley-VCH, Weinheim, Germany **2010**.
- [25] J. R. Whitlock, A. J. Heynen, M. G. Shuler, M. F. Bear, *Science* **2006**, 313, 1093.
- [26] E. R. Kandel, J. H. Schwartz, T. M. Jessell, in *Principles of Neural Science*, 4th ed., (Ed: E. R. Kandel, J. H. Schwartz, T. M. Jessell) McGraw-Hill, New York **2000**.
- [27] R. C. Atkinson, R. M. Shiffrin, in *The Psychology of Learning and Motivation: Advances in Research and Theory*, Vol. 2, (Eds: K. W. Spence, J. T. Spence), Academic Press, New York **1968**, pp. 89–195.
- [28] A. Nayak, T. Tsuruoka, K. Terabe, T. Hasegawa, M. Aono, *Nanotechnology* **2011**, 22, 235201.
- [29] M. Kundu, T. Hasegawa, K. Terabe, M. Aono, *J. Appl. Phys.* **2008**, 103, 073523.
- [30] T. Tani, in *Photographic Sensitivity: Theory and Mechanisms*, (Ed: M. Lapp, J.-I. Nishizawa, B. B. Snively, H. Stark, A. C. Tam, T. Wilson), Oxford University Press, New York **1995**.
- [31] D. C. Rubin, A. E. Wenzel, *Psychol. Rev.* **1996**, 103, 734.
- [32] T. Tamura, T. Hasegawa, K. Terabe, T. Nakayama, T. Sakamoto, H. Sunamura, H. Kawaura, S. Hosaka, M. Aono, *J. Phys.: Conf. Ser.* **2007**, 61, 1157.
- [33] A. Nayak, T. Tamura, T. Tsuruoka, K. Terabe, S. Hosaka, T. Hasegawa, M. Aono, *J. Phys. Chem. Lett.* **2010**, 1, 604.
- [34] M. Morales-Masis, S. J. van der Molen, T. Hasegawa, J. M. van Ruitenbeek, *Phys. Rev. B* **2011**, 84, 115310.
- [35] J. Urban, H. Sack-Kongehl, K. Weiss, *Z. Phys. D* **1996**, 36, 73.
- [36] H. Ruuska, A. P. Tapani, *J. Phys. Chem. B* **2004**, 108, 2614.
- [37] H. Gronbeck, M. Andersson, A. Rosen, *Nanostruct. Mater.* **1995**, 5, 193.
- [38] S. Maupai, M. Stratmann, A. S. Dakkouria, *Electrochem. Solid-State Lett.* **2002**, 5, C35.
- [39] A. Nayak, T. Tsuruoka, K. Terabe, T. Hasegawa, M. Aono, *Appl. Phys. Lett.* **2011**, 98, 233501.
- [40] S. J. Schiff, G. G. Somjen, *Brain Res.* **1985**, 345, 279.
- [41] J. C. Montgomery, J. A. Macdonald, *Am. J. Physiol. - Reg. I.* **1990**, 259, R191.
- [42] V. A. Klyachko, C. F. Stevens, *J. Neurosci.* **2006**, 26, 6945.